Bose-Einstein condensation for trapped atomic polaritons in a biconical waveguide cavity

I. Yu. Chestnov, A. P. Alodjants,* and S. M. Arakelian
Department of Physics and Applied Mathematics, Vladimir State University named after A. G. and N. G. Stoletovs, Gorky str. 87, 600000, Vladimir, Russia

J. Klaers, F. Vewinger, and M. Weitz
Institut fur Angewandte Physik der Universität Bonn, Wegelerstraße 8, 53115 Bonn, Germany
(Received 7 March 2012; published 31 May 2012)

We study the problem of high-temperature Bose-Einstein condensation (BEC) of atom-light polaritons in a waveguide cavity appearing due to the interaction of two-level atoms with (nonresonant) quantized optical radiation in the strong-coupling regime and in the presence of optical collisions (OCs) with buffer-gas particles. Specifically, we propose a special biconical waveguide cavity (BWC), permitting localization and trapping of low-branch (LB) polaritons imposed by the variation of the waveguide radius in longitudinal direction. We have shown that the critical temperature of BEC occurring in the system can be high enough—a few hundred kelvins; it is connected with the photonlike character of LB polaritons and strongly depends on waveguide-cavity parameters. In the case of a linear trapping potential we obtain an Airy-shaped polariton condensate wave function which, when disturbed out of equilibrium, exhibits small-amplitude oscillations with the characteristic period in the picosecond domain.

DOI: 10.1103/PhysRevA.85.053648 PACS number(s): 67.85.Jk, 05.30.Jp, 42.82.Et, 42.50.Ct

I. INTRODUCTION

The investigation of quantum and statistical properties of Bose-gases in low and especially in one dimension (1D) has evoked indefatigable interest in atomic optics and condensed matter physics for the last few decades (see, e.g., [1–6]). In particular, at finite temperatures for a 1D or two-dimensional (2D) ideal Bose gas, a true Bose-Einstein condensation (BEC) can only be reached in the presence of a suitable trapping potential [4], and the critical temperature for the phase transition depends on the shape of the trapping potential, which is usually harmonic in practice (cf. [3,4]). Low-dimensional systems have been studied using atoms in highly deformed traps [7] where effects of dimensional reduction become important [8]. Alternative systems are bosonic quasiparticles, where light and matter are coupled in a coherent way (see, e.g., [9]). Here quantum and statistical properties of light Bose-quasiparticles, like excitons [10], magnons [11], and polaritons (see, e.g., [12–15]) have been considered. For example, exciton-polaritons occurring in quantum well structures placed in microcavities can be treated as a *2D gas* of bosonic particles having an effective mass which is many orders smaller than the mass of an electron in vacuum. This allows us to study relatively high-temperature phase transitions in low-dimensional bosonic systems. Recently, evidence of a Kosterlitz-Thouless phase transition (cf. [2]) superfluid behavior of exciton-polaritons in such systems has been reported by many labs [12,13]. However, in current semiconductor structures the thermalization time is in the picosecond domain and comparable with the particle lifetime; thus we deal here with nonequilibrium "condensates" [14], for which dissipative and optical pumping effects play a crucial role (cf. [15]). The characteristic temperatures for these condensates are a few tens of kelvins, which is far above the temperature of atomic condensates, but still far below room temperature.

Recently, room-temperature Bose-Einstein-condensation of photons has been observed [16,17], where the photons are confined in a 2D curved-mirror optical microresonator filled with a dye solution. Thermalization of the photon gas is established by thermal contact between the photons and the dye solution, using repeated absorption and reemission processes in the dye solution [18]. Frequent collisions, on a timescale much faster than the excited-state lifetime, lead to a decoupling of photons and dye molecules, thus the relevant particles are not polaritons but photons [16,17] in these experiments.

In the present paper we discuss a different approach to reach a high (room and beyond) temperature phase transition with mixed matter-field states—polaritons in an atomic medium. In particular, dressed-sate polaritons, where a light field is coherently and strongly coupled to a two-level atom, leading to a bosonic quasiparticle (in a suitable limit) are attractive candidates due to their potentially longer lifetime (cf. [19,20]). In this system thermal equilibrium of coupled atom-light (dressed) states can be achieved experimentally within a nanosecond domain and is limited by the natural lifetime of the two-level atoms. Here, optical collisions (OCs) with buffer-gas atoms can lead to thermalization; experimental evidence for a thermal quasi-equilibrium of coupled atom-light states has been found [21,22]. The obtained thermalization time has been about ten times shorter than the natural lifetime at full optical power. Here, the limited available power in the light field prevented a full thermalization. To overcome this problem, in Refs. [23,24] special metallic waveguides of various configurations with a length up to a few millimeters have been considered for trapping the polaritons, similar to waveguides and closed resonators examined for the confinement of microwave irradiation (cf. [25,26]). The lifetime of photonlike polaritons trapped in the waveguide can be longer than the thermalization time and is mainly

*alodjants@vlsu.ru

determined by the cavity Q factor. Thus we expect in such a waveguide that, for a large and negative atom-field detuning, a high-temperature phase transition to a superradiant state of the polaritons can be reached [24].

In this paper we study thermodynamic and critical properties of dressed-state polaritons trapped in a biconical waveguide (i.e., metallic microtubes with different geometries [27]). In this case one can study the thermodynamics of a 1D quantum gas, which exhibits a high-temperature phase transition to a BEC in the case of a trapping potential which is more confining than harmonic [3]. For this reason we consider waveguides with a biconical shape, which leads to a trapping potential in the propagation direction. Throughout the paper, we assume the strong-coupling limit; that is, the eigenstates of the coupled atom-light system are treated as polaritons. In Sec. II we describe the waveguide-cavity model for confinement of the optical mode. To be more specific, we consider field properties in an empty lossless metallic biconical waveguide cavity (BWC) where photons are confined in transversal and trapped in longitudinal dimension. In Sec. III we give a quantum description of the atom-field interaction in the waveguide, and the problem of specifying waveguide parameters in the limit of weak trapping is considered. Thermodynamic properties of the 1D ideal gas of photonlike polaritons are examined, where we find a phase transition to a BEC state at experimentally feasible temperatures. In Sec. IV we discuss the dynamical properties of condensed LB polaritons. In the conclusion, we summarize the results obtained.

II. BICONICAL WAVEGUIDE CAVITY

We start by describing the problem of photon trapping in the empty BWC, sketched in Fig. 1. We assume metallic boundary conditions, and for the case of simplicity the cavity is assumed to be lossless. The radius of the cylindrically symmetric waveguide depends on z following

$$R(z) = \frac{R_0}{F(|z|)}, \tag{1}$$

with $F(0) = 1$ and $F(|z|)$ being a function increasing monotonically with $|z|$ (i.e., $\partial F/\partial z > 0$ for $z > 0$), similar to bottle resonators based on glass materials (and with relatively large diameter); see Ref. [23]. Here, we focus on waveguides with a maximal diameter that is close to the wavelength of the optical field. In this limit it is possible to guarantee a

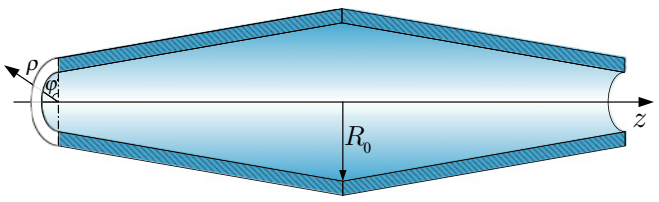

FIG. 1. (Color online) Biconical waveguide for photon (and polariton) trapping. Shown is a waveguide with a radius variation following the form $R(z) = R_0(1 - \alpha|z|)$, which is obtained from Eq. (13) for $\nu = 1$ in the limit of a small value of α. In this case the radius variation within the limited waveguide length is roughly linear. The radius at the waveguide center $z = 0$ is taken to be close to $\lambda/2.61$, yielding a low-frequency cutoff close to the atomic resonance.

spacing of the transverse modes above the thermal energy, which allows for the transverse mode quantum numbers to be frozen. The system becomes effectively one dimensional, with a continuum of longitudinal modes above a low-frequency cutoff. For a suitable density of states, BEC then becomes possible in this one-dimensional situation. For a related although two-dimensional situation, see Ref. [17]. We consider biconical waveguides, because fabrication of a conical hole can be done by, for example, ion beam etching or laser drilling, and then two of those holes can be combined to get the required cavity. Alternatively, self-assembling nanotubes can be used, which have been shown to be suitable for implementation in the experiment [23].

We use the adiabatic approximation, assuming that $R(z)$ is slowly varying with the z coordinate; that is, that the condition

$$\left|\frac{dR(z)}{dz}\right| \ll 1 \tag{2}$$

is fulfilled. In other words, we suppose that the angle between waveguide and z axis is small throughout the length of the waveguide—see Fig. 1.

The field properties in such a system can be described by the wave (scalar Helmholtz) equation for the vector potential $\Phi(x,y,z)$ (we consider *TM modes* of polarization only; cf. [28]):

$$\Delta\Phi(x,y,z) + k^2\Phi(x,y,z) = 0, \tag{3}$$

where we assume that the field evolves in time as $e^{i\omega t}$, and $k = \omega/c$ is the wave vector. We can interpret $\Phi(x,y,z) \equiv \Phi_l(x,y,z)$ as a photonic wave function in the waveguide, where the index l numerates a set of quantum numbers corresponding to the solution of Eq. (3) in terms of special functions.

Both electric (E_ρ, E_φ, and E_z) and magnetic (H_ρ, H_φ, and H_z) field components can be found by using standard expressions for the $\Phi(x,y,z)$-function derivatives in cylindrical coordinates (see, e.g., [28]). For TM modes the z component of the magnetic field is $H_z = 0$, and the metallic boundary condition imposes that the electric field E has only a normal component on the waveguide surface.

Taking into account axial symmetry of the waveguide in Fig. 1 it is efficient to rewrite Eq. (3) in cylindrical coordinates z, ρ, and φ as

$$\frac{1}{\rho}\frac{\partial}{\partial\rho}\left(\rho\frac{\partial\Phi}{\partial\rho}\right) + \frac{\partial^2\Phi}{\partial z^2} + \frac{1}{\rho^2}\frac{\partial^2\Phi}{\partial\varphi^2} + k^2\Phi = 0, \tag{4}$$

where the wave vector k is defined as

$$k^2 = k_\perp^2 + k_z^2. \tag{5}$$

We are looking for the solution of Eq. (4) in the form

$$\Phi(\rho,z,\varphi) = \Psi(z)\Theta(\rho,z)e^{im\varphi}, \tag{6}$$

where m is an integer (azimuthal quantum) number, and the functions $\Theta(\rho,z)$ and $\Psi(z)$ comply with the equations

$$\frac{\partial^2\Theta}{\partial\rho^2} + \frac{1}{\rho}\frac{\partial\Theta}{\partial\rho} + \left[k_\perp^2(z) - \frac{m^2}{\rho^2}\right]\Theta = 0, \tag{7}$$

$$\frac{\partial^2\Psi(z)}{\partial z^2} + k_z^2\Psi(z) = 0. \tag{8}$$

In Eq. (7) the terms containing derivatives of the longitudinal coordinate z are omitted due to the adiabaticity condition (2).

The solution for the radial distribution $\Theta(\rho,z)$ can be expressed in terms of Bessel functions,

$$\Theta(\rho,z) = J_m(k_\perp \rho), \tag{9}$$

where the wave-vector component $k_\perp$ is quantized in this case. Omitting lengthy but straightforward calculations for the $k_\perp$ component of the wave vector for TM modes in the waveguide, we obtain

$$k_{\perp,mp}(z) = \frac{g_{mp}}{R(z)} = k^{(0)}_{\perp,mp} F\left(|z|\right), \tag{10}$$

where $k^{(0)}_{\perp,mp} = g_{mp}/R_0$ is a transversal wave vector component, g_{mp} is the pth zero of the Bessel function $J_m(x)$ of the mth order [29]. In Eq. (10) we have used the metallic boundary conditions for electric field components, $J_m(k_\perp R(z)) = 0$. For $p = 1$ and $m = 0$ we find the cavity transverse ground state mode, yielding $k_{\perp,01}(z) = g_{01}/R(z)$ with $g_{01} \approx 2.405$.

Equation (5) implies a dispersion relation of the form

$$\omega_{\rm ph} = ck = c\sqrt{\left[k^{(0)}_{\perp,mp} F(|z|)\right]^2 + k_z^2}.$$

In the approximation $k_{\perp,mp}(z) \gg k_z$ we arrive at

$$\omega_{\rm ph} \simeq ck^{(0)}_{\perp,mp} F(|z|) + \frac{ck_z^2}{2k^{(0)}_{\perp,mp} F\left(|z|\right)}. \tag{11}$$

In this limit the second term is much smaller than the first term and we assume that, in the smaller, kinetic energy term we can set $F(|z|) = 1$. This approximation is valid in the limit of a not-too-large overall variation in the diameter of the waveguide. We arrive at a photon energy in the BWC

$$E_{\rm ph} = m_{\rm ph}c^2 + \frac{(\hbar k_z)^2}{2m_{\rm ph}} + V_{\rm ph}(z), \tag{12}$$

where we have defined an effective photon mass $m_{\rm ph} = \hbar k^{(0)}_{\perp,mp}/c$ (with $\omega_{\rm cutoff} = m_{\rm ph}c^2/\hbar$ as the low-frequency cutoff) and an effective photon-trapping potential $V_{\rm ph}(z) = \hbar c k^{(0)}_\perp [F(|z|) - 1]$ in analogy with Ref. [17]. The system becomes formally equivalent to a one-dimensional ideal gas of massive particles moving along the z axis under confinement in the potential $V_{\rm ph}(z)$.

In the following we assume a dependence

$$F(|z|) = 1 + \alpha\,|z|^\nu\,, \tag{13}$$

corresponding to a waveguide diameter variation along the z axis of $R(z) = R_0/(1 + \alpha|z|^\nu)$; with $\nu > 0$ and $\alpha > 0$, we arrive at a potential of the form $V_{\rm ph}(z) = \hbar c k^{(0)}_\perp \alpha|z|^\nu = m_{\rm ph}c^2\alpha|z|^\nu$. True BEC is expected to be possible in the 1D system if the potential is more confining than parabolic (i.e., $\nu < 2$ [3]). We here mostly are interested in the case of $\nu = 1$, for which $R(z) = R_0/(1 + \alpha|z|)$, which yields a linear trapping potential following $V_{\rm ph}(z) = m_{\rm ph}c^2\alpha|z|$ (see Fig. 1). For the case of a relatively small variation of the waveguide diameter over the length l of the waveguide (i.e., $\frac{1}{2}\alpha l \ll 1$), one may use a linear variation of the diameter $R(z) \approx R_0(1 - \alpha|z|)$, which gives the desired potential in the first-order approximation [23]. Such a purely biconical design can be easier to fabricate experimentally.

Given the dispersion relation (12), the longitudinal wave function $\Psi(z)$ [Eq. (8)], follows the Schrödinger equation

$$\frac{\partial^2\Psi(z)}{\partial z^2} + \frac{2m_{\rm ph}}{\hbar^2}(E - U_{\rm ph}|z|^\nu)\Psi(z) = 0, \tag{14}$$

where $E = E_{\rm ph} - m_{\rm ph}c^2$ is the shifted photon energy in the cavity, and we made the definition $U_{\rm ph} = m_{\rm ph}c^2\alpha$.

The solutions $\Psi_n(z)$ of the Schrödinger equation (14) can be given in terms of special functions (see, e.g., [29]). In the quasiclassical approach the energy spectrum of photonic field in the waveguide can be obtained from familiar Bohr-Sommerfeld quantization principle and reads (see, e.g., [30])

$$E_n = \hbar\omega_\nu (n + 1/2)^{2\nu/(\nu+2)}, \tag{15}$$

with the characteristic frequency of photonic "particle" oscillation (i.e., trapping frequency) in the cavity

$$\omega_\nu = \left(\frac{\pi U_{\rm ph}^{1/\nu}}{2^{3/2} m_{\rm ph}^{1/2}\hbar^{(2-\nu)/2\nu} I(\nu)}\right)^{2\nu/(\nu+2)}. \tag{16}$$

Here we have defined $I(\nu) = \int_0^1 (1 - |t|^\nu)^{1/2} dt$.

A characteristic length for the waveguide cavity can be obtained by looking at the turning points $z = \pm z_c$ for the photonic ground-state mode, given by

$$z_c = (E/U_{ph})^{1/\nu} = \left(\frac{\pi}{4I(\nu)}\right)^{\frac{2}{2+\nu}} d_\nu, \tag{17}$$

where $d_\nu = [\hbar^2/(2m_{ph}^2c^2\alpha)]^{1/(\nu+2)}$ defines a characteristic longitudinal scale of localization of the ground state ($n = 0$). From this we can define the condition for the validity of the quasiclassical approach, given as (cf. [31])

$$k_z d_\nu \gg (\nu/2)^{1/3}. \tag{18}$$

Relation (18) can be satisfied for a given k_z by adjusting the waveguide parameter α [cf. (2)].

III. THERMODYNAMICS OF POLARITONS IN WAVEGUIDE CAVITY

The description of atomic polaritons in a small-volume cavity can be given in a similar way as represented in Refs. [20,24]; namely, by using Holstein-Primakoff transformation for atomic excitations. The Hamiltonian of the total system of atom and quantized field is given by $H = H_{\rm rad} + H_{\rm at} + H_{\rm int}$, where $H_{\rm rad}$ characterizes noninteracting photons in the waveguide, $H_{\rm at}$ is the Hamiltonian of the atomic ensemble, and $H_{\rm int}$ is responsible for the interaction of $N_{\rm at}$ two-level atoms with the quantized optical field in the cavity. In momentum representation the Hamiltonian H may be written as

$$H = \hbar\sum_{\vec{k}}[\omega_{\rm ph}\hat{f}^\dagger_{\vec{k}}\hat{f}_{\vec{k}} + \omega_{\rm at}\hat{\phi}^\dagger_{\vec{k}}\hat{\phi}_{\vec{k}} + \kappa(\hat{f}^\dagger_{\vec{k}}\hat{\phi}_{\vec{k}} + \hat{\phi}^\dagger_{\vec{k}}\hat{f}_{\vec{k}})] - \frac{\hbar\kappa}{2N_{\rm at}}\sum_{kk'q}(\hat{f}^\dagger_{k+q}\hat{\phi}^\dagger_{k'-q}\hat{\phi}_k\hat{\phi}_{k'} + \hat{\phi}^\dagger_k\hat{\phi}^\dagger_{k'}\hat{\phi}_{k'-q}\hat{f}_{k+q}), \tag{19}$$

where $\hat{f}_{\vec{k}}$ ($\hat{f}^\dagger_{\vec{k}}$) is the annihilation (creation) operator for the photons absorbed (emitted), $\hat{\phi}_{\vec{k}}$ ($\hat{\phi}^\dagger_{\vec{k}}$) is the annihilation

(creation) operator that characterizes excitations (polarization) of a two-level atomic ensemble and obeys usual commutation relation for a Bose system,

$$\kappa = \left(\frac{|\wp_{ab}|^2 \omega_L N_{\rm at}}{2\hbar\varepsilon_0 V_M} \right)^{1/2}$$

is the collective atom-field interaction strength, $\wp_{ab}$ is atomic dipole matrix element, V_M is an effective volume of mode occupation within the region of atom-field interaction that can be defined as

$$V_M = \int_{\rm cavity} \frac{|\Phi(r)|^2}{\max[|\Phi(r)|^2]} d^3r,$$

where $\max[|\Phi(r)|^2]$ is maximal value of the square of the wave function (cf. [24,32]). Here we have assumed that the dipole matrix element $\wp_{ab}$ is independent of the mode. This simplification is justified because the exact transition rates do not influence the thermodynamic properties of the system. The nonlinear part of the Hamiltonian H [i.e., the last term in Eq. (19)] characterizes two-body polariton interaction processes due to atomic saturation effects. The polaritonic dispersion is determined by the photon dispersion $\omega_{\rm ph}(k)$ and the atomic excitation dispersion, which is described by

$$\omega_{\rm at} \equiv \omega_{\rm at}(k) = \omega_0 + \frac{\hbar k_z^2}{2m_{\rm at}}, \tag{20}$$

where ω_0 is the atomic transition frequency.

If a quantum field intensity is not too high (the number of photons is essentially smaller than the number of atoms), we can assume that the corresponding dispersion relation for polariton states is not modified compared to the uncoupled case. Thus, we can use a polariton basis to diagonalize the total Hamiltonian in Eq. (19) by using the unitary transformation

$$\hat{\Xi}_{1,\vec{k}} = X_k \hat{f}_{\vec{k}} + C_k \hat{\phi}_k, \tag{21a}$$

$$\hat{\Xi}_{2,\vec{k}} = X_k \hat{\phi}_k - C_k \hat{f}_{\vec{k}}, \tag{21b}$$

where the introduced annihilation operators $\hat{\Xi}_{1,\vec{k}}$, $\hat{\Xi}_{2,\vec{k}}$ characterize polaritons in the atomic medium, corresponding to two types of elementary excitations which, in the low-density limit, satisfy the usual boson commutation relations (cf. [24]). Parameters X_k and C_k are real Hopfield coefficients satisfying the condition $X_k^2 + C_k^2 = 1$, which determines the contribution of the photon (C_k) and atomic excitation (X_k) fraction to the polariton annihilation operators (21) according to

$$X_k = \frac{1}{\sqrt{2}} \left(1 + \frac{\delta_k}{\sqrt{4\kappa^2 + \delta_k^2}} \right)^{1/2}, \tag{22a}$$

$$C_k = \frac{1}{\sqrt{2}} \left(1 - \frac{\delta_k}{\sqrt{4\kappa^2 + \delta_k^2}} \right)^{1/2}, \tag{22b}$$

where

$$\delta_k = \omega_{\rm ph} - \omega_{\rm at} \approx \Delta + \frac{\hbar k_z^2}{2m_{\rm ph}} + \frac{V_{\rm ph}(z)}{\hbar}$$

is the frequency mismatch. Here $\Delta = \omega_{\rm L} - \omega_0$ is the atom-field detuning, where ω_L is the laser-light frequency which is taken to be close to $\omega_{\rm cutoff}$. In the presence of photon trapping, the X_k and C_k parameters depend on the waveguide longitudinal coordinate z.

We confine our analysis to polaritons of the lower branch (LB polaritons), and we ignore the effects of interactions between the lower and upper polariton branches. Taking into account the quasiclassical approach [cf. Eq. (18)] for the photonic field in the BWC, we find the general conditions for the observation of a BEC of (lower branch) polaritons,

$$\Delta E_n \ll k_B T \ll \hbar\Omega_{R0}, \tag{23}$$

where $\Omega_{R0} = (\Delta^2 + 4\kappa^2)^{1/2}$ is the *zero-momentum* Rabi splitting frequency between the lower and upper polariton branch. The first constraint in Eq. (23) represents the condition for a quasiclassical limit where the energy spacing $\Delta E_n \sim \hbar\omega_v$ [see Eq. (15)] of the quantized photonic states is essentially smaller than the thermal energy and the states may be treated as a continuum (cf. [3]), where the energy levels are populated according to a Bose-Einstein distribution in thermal equilibrium. The second condition implies that the thermal energy is not enough to excite lower branch polaritons to the upper branch, essentially allowing us to neglect the upper branch.

Taking Eqs. (21) and (22) into account from Eq. (19) we can obtain the LB Hamiltonian $H_{\rm LB}$ in the form

$$H_{\rm LB} = \hbar \sum_{\vec{k}} \Omega_{\vec{k}} \hat{\Xi}^\dagger_{2,\vec{k}} \hat{\Xi}_{2,\vec{k}} + \sum_{kk'q} U_{\vec{k}\vec{k}'\vec{q}} \hat{\Xi}^\dagger_{2,k+q} \hat{\Xi}^\dagger_{2,k'-q} \hat{\Xi}_{2,k} \hat{\Xi}_{2,k'}, \tag{24}$$

where $\Omega_{\vec{k}} = \frac{1}{2}(\omega_{\rm at} + \omega_{\rm ph} - \Omega_R)$ determines the dispersion relation for LB polaritons; $\Omega_R = (\delta^2 + 4\kappa^2)^{1/2}$ is the Rabi splitting frequency that determines the gap between upper and lower states. The gap is minimal and equal to Ω_{R0} taken for $k_z = 0$ at the center of the trap (waveguide) at $z = 0$. In Eq. (24), we use the definition

$$U_{\vec{k}\vec{k}'\vec{q}} = \frac{\hbar\kappa}{2N_{\rm at}} (C_{|\vec{k}+\vec{q}|} X_{\vec{k}'} + C_{\vec{k}'} X_{|\vec{k}+\vec{q}|}) X_{|\vec{k}'-\vec{q}|} X_{\vec{k}},$$

which determines two-body polariton-polariton scattering processes. The effective mass of the LB polaritons is found to be

$$m_{\rm pol} \equiv \hbar \left(\frac{\partial^2 \Omega_{\vec{k}}}{\partial k_z^2} \bigg|_{k_z=0} \right)^{-1} = \frac{2m_{\rm at} m_{\rm ph} \Omega_{Rz}(z)}{(m_{\rm at} + m_{\rm ph})\Omega_{Rz}(z) - (m_{\rm at} - m_{\rm ph})[\Delta + V_{\rm ph}(z)/\hbar]}, \tag{25}$$

where $\Omega_{Rz}(z) = \{[\Delta + V_{\rm ph}(z)/\hbar]^2 + 4\kappa^2\}^{1/2}$ is the z-dependent Rabi splitting frequency.

To be more specific we examine the interaction between a quantized field and rubidium atoms, which are treated as a two-level system. The transition frequency is taken as the weighted mean of the rubidium D lines, $\omega_0/(2\pi) \simeq 382$ THz, and the laser is taken to be red detuned by $|\Delta|/(2\pi) \geqslant 11$ THz, $\Delta < 0$ [21,22]. In the experiments reported, the thermal energy ($k_B T$) for the atoms at ambient temperatures ($T = 530$ K) is about the frequency of the Rabi splitting $\Omega_{R0}/(2\pi) \simeq 11$ THz in energy units, thus condition (23) has not been completely

achieved yet [21–24]. We consider the perturbative limit when $\Omega_0,\ \kappa \ll |\Delta|$; that is, $\Omega_{R0}/(2\pi) \approx |\Delta|/(2\pi) \geqslant 11$ THz. For negative detuning ($\Delta < 0$) the LB polaritons with relatively small momentum k_z at the center of the trap are photonlike with mass

$$m_{\rm pol} \approx m_{\rm ph}\frac{2\Omega_{R0}}{\Omega_{R0}+|\Delta|} \simeq 2.8\times 10^{-36}\ {\rm kg};$$

that is, $\delta_k \simeq \Delta$, $X_k \approx 0$, $C_k \approx 1$, and $\hat{\Xi}_{2,\vec{k}} \simeq -\hat{f}_{\vec{k}}$ (cf. [24]).

The role of polariton-polariton scattering processes in Eq. (24) is negligibly small in this limit. At the bottom of the dispersion curve the polariton scattering parameter $U_0 \equiv U_{\vec{k}\vec{k}'\vec{q}}|_{\vec{k}\vec{k}'\vec{q}=0}$ behaves like $U_0 \simeq \hbar\kappa^4/(N_{\rm at}|\Delta|^3)$. Hence in the limit of a large atom-light detuning $|\Delta|$ (ratio $\kappa/|\Delta|$ is about 0.057, cf. [22,24]) and for a macroscopically large number of atoms ($N_{\rm at} \gg 1$) the gas of LB polaritons can be treated as ideal.

The photonic fraction of the LB polaritons—Hopfield coefficient $C_0^2 \equiv C_{k_z=0}^2$—and the mass of LB polaritons $m_{\rm pol}$ taken in the limit of zero momentum $k_z = 0$ as a function of z are presented in Figs. 2(a) and 2(b). With increasing coordinate z, LB polaritons become more atom like and present half-matter–half-photon quasiparticles [$X_0(z) = C_0(z) = 2^{-1/2}$] with mass

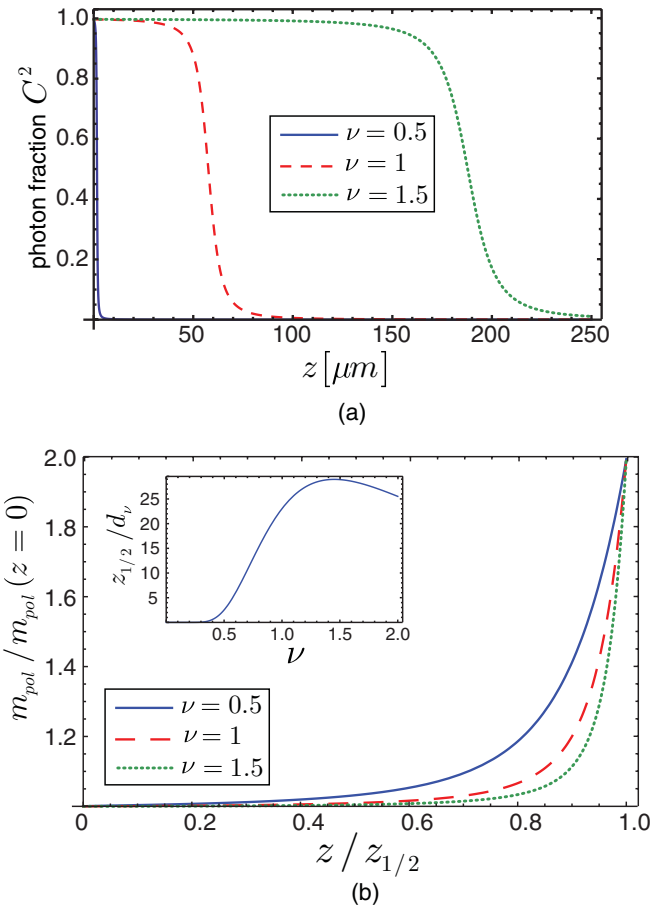

FIG. 2. (Color online) (a) Polariton photon fraction (coefficient C_0^2) and (b) normalized LB polariton mass $m_{\rm pol}$ as a function of z for trapping-power parameter $\nu = 0.5,\ 1,\ 1.5$. The inset shows the dependence of $z_{1/2}/d_\nu$ versus parameter ν. The parameters are $\Delta/2\pi = -11$ THz, $R_0 \simeq \lambda/2.61 \approx 0.3\ \mu$m, and $\alpha^{1/\nu} = 0.0005\ \mu{\rm m}^{-1}$.

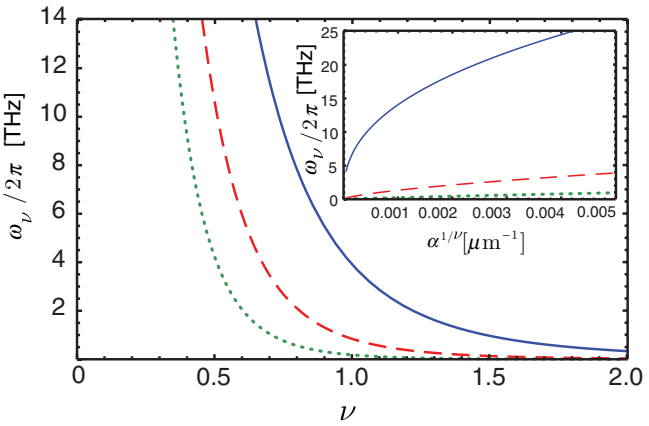

FIG. 3. (Color online) Dependencies of photonic trapping frequency $\omega_\nu/(2\pi)$ versus trapping parameter ν. Blue solid line corresponds to $\alpha^{1/\nu} = 0.005\ \mu{\rm m}^{-1}$, red dashed line to $\alpha^{1/\nu} = 0.0005\ \mu{\rm m}^{-1}$, green dotted line to $\alpha^{1/\nu} = 0.000\,05\ \mu{\rm m}^{-1}$. In the inset the dependence of ω_ν versus the parameter $\alpha^{1/\nu}$ for $\nu = 0.5$ (blue solid line), $\nu = 1$ (red dashed line), and $\nu = 1.5$ (green dotted line) is depicted.

$m_{\rm pol} \approx 2m_{\rm ph}$ at the distance $z_{1/2} = (\hbar|\Delta|/U_{\rm ph})^{1/\nu}$, where photonic and atomic dispersion lines cross [see Fig. 4(a)]. From definition (25) it follows that the mass of polaritons becomes z independent if condition $V_{\rm ph}(z) \ll \hbar|\Delta|$ is satisfied. Since $V_{\rm ph}(d_\nu) \sim \hbar\omega_\nu$, the inequalities (23) already involve the above condition. In this limit an effective width of the photonic mode localization d_ν is essentially smaller than the characteristic length $z_{1/2}$. The ratio $z_{1/2}/d_\nu$ for different trapping power is outlined in the inset in Fig. 2(b). For $\nu = 1$ the region of photon mode localization is more than ten times shorter than characteristic length $z_{1/2}$, allowing us to treat the LB polaritons as nearly photonic. The variation of the polariton mass [see Fig. 2(b)] is small for $z \ll z_{1/2}$ [i.e., under condition (23)], allowing us to treat the LB polaritons as particles with constant mass.

Figure 3 shows the characteristic trapping frequency ω_ν as a function of parameter ν for the cavity, where the red (dashed) curve corresponds to the waveguide α parameter used in Fig. 2. For $\nu \geqslant 1$ the condition (23) can be fulfilled for any reasonable value of α parameter by choosing the atom-field detuning $|\Delta|$. On the other hand, ω_ν increases within the domain of $0 < \nu < 1$ and the fulfillment of condition (23) mainly depends on the given value of curvature of the waveguide radius (i.e., on the α parameter) and on the experimentally accessible atom-field detuning $|\Delta|$.

The results for the rubidium system allow us to further simplify the Hamiltonian for the LB polaritons: At small momenta $\hbar k_z^2/(2m_{\rm pol}) \ll \Omega_{R0}$ it approaches

$$H_{\rm LB} \approx \sum_{\vec{k}}\left[\frac{\hbar^2 k_z^2}{2m_{\rm pol}} + U(z)\right]\hat{\Xi}_{\vec{k}}^\dagger\hat{\Xi}_{\vec{k}}, \tag{26}$$

where $U(z)$ is an effective trapping potential for polaritons defined as

$$U(z) = \tfrac{1}{2}\{V_{\rm ph}(z) - \sqrt{[\hbar\Delta + V_{\rm ph}(z)]^2 + 4\hbar^2\kappa^2} + \hbar\Omega_{R0}\}. \tag{27}$$

The last term in curly brackets of Eq. (27) specifies the minimal level of potential energy $U(z)$, which is equal to zero $[U(z)|_{z=0} = 0]$, at the center of the trap. From Eq. (27) under the condition (23) for photonlike polaritons one can obtain a simple expression for a power-law potential

$$U(z) \simeq U_{\rm pol}\,|z|^{\nu}\,, \tag{28}$$

where $U_{\rm pol} = m_{\rm ph}c^2\alpha(\Omega_{R0} + |\Delta|)/(2\Omega_{R0})$.

Let us examine the statistical properties of LB polaritons trapped in the waveguide. From the above discussion, we can treat the polaritons as one-dimensional ideal bosons confined in the potential $U(z)$. In the quasiclassical approximation (23) the density of states approaches

$$\rho\,(\varepsilon) = \frac{\sqrt{2}}{\pi\hbar}\int_0^{l(\varepsilon)}\left(\frac{m_{\rm pol}}{\varepsilon - U(z)}\right)^{1/2} dz, \tag{29}$$

where $l(\varepsilon) = (\varepsilon/U_{\rm pol})^{1/\nu}$ is a characteristic length of localization for LB polaritons with energy ε [see Fig. 4(a)]. The density of states $\rho(\varepsilon)$ as a function of the normalized polariton energy $\varepsilon/(\hbar|\Delta|)$ is plotted in Fig. 4(b) for the approximate (dashed) and exact (solid) potential. Differences occur at polariton energies of $\varepsilon \sim \hbar|\Delta|$; that is, for LB polaritons weakly confined inside the region $z < z_{1/2}$, one can use the power-law approximation (28) of the trapping potential $U(z)$.

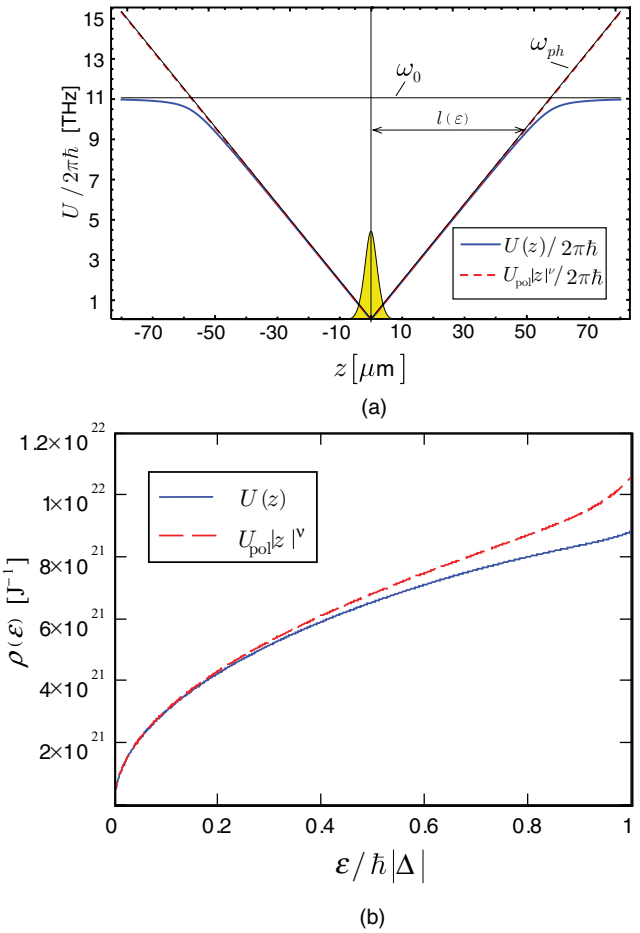

FIG. 4. (Color online) (a) Energy of polariton trapping versus coordinate z taken for $\nu = 1$. (b) Dependence of density of states $\rho(\varepsilon)$ on normalized polariton energy $\varepsilon/(\hbar|\Delta|)$. The solid curves correspond to the exact trapping potential(27), and the dashed curves are relevant to the power-law potential (28). The black solid lines correspond to atomic $\omega_{\rm at}$ and photonic $\omega_{\rm ph}$ frequencies. The shaded (yellow) area corresponds to LB polariton ground-state wave function (see Sec. IV).

The total number of LB polaritons $N_{\rm pol}$ is given by

$$N_{\rm pol} = N_0 + \int \frac{\rho(\varepsilon)d\varepsilon}{\exp[(\varepsilon-\mu)/k_BT] - 1}, \tag{30}$$

where N_0 is the number of ground-state polaritons and μ is the chemical potential.

We find the critical temperature T_C for which the ground-state occupation becomes macroscopic by solving Eq. (30) at $\mu = 0$. For the onset of Bose-Einstein condensation one finds (cf. [3])

$$k_BT_C = \left[\frac{\pi\hbar N_{\rm pol}\nu U_{\rm pol}^{1/\nu}}{\sqrt{2m_{\rm pol}}F(\nu)\Gamma(x)\zeta(x)}\right]^{2\nu/(2+\nu)}, \tag{31}$$

where

$$F(\nu) = \int_0^1 \frac{t^{1/\nu-1}dt}{\sqrt{1-t}},$$

and $\Gamma(x)$ and $\zeta(x)$ are the gamma and the Riemann (zeta) functions, respectively, taken at $x = 1/\nu + 1/2$. Below the critical temperature the occupation of the ground state is determined by

$$N_0 = N_{\rm pol}\left[1 - \left(\frac{T}{T_C}\right)^{1/\nu+1/2}\right]. \tag{32}$$

In the experiment, the average number of LB polaritons, $N_{\rm pol} = \sum_{\vec{k}}\langle\hat{\Xi}_{\vec{k}}^{\dagger}\hat{\Xi}_{\vec{k}}\rangle \approx N_{\rm ph}$, can be estimated using the photonlike character of polaritons in the perturbation limit. Notice that a polaritonic model is valid under the low-excitation-density limit for which the average number of photons $N_{\rm ph}$ is essentially smaller than the average number of atoms $N_{\rm at}$. Using experimentally accessible rubidium atom densities, which are $n_{\rm at} = N_{\rm at}/V_M = 10^{16}$ cm^{-3}, (cf. [21]) and taking the occupation volume V_M of the lowest photonic mode (TM$_{01}$ mode) to be $V_M \approx 0.5\ \mu$m^3 we find an average number of $N_{\rm at} = 5000$ atoms in the BWC, thus limiting the experiment to a few hundred polaritons. In Fig. 5 the critical temperature

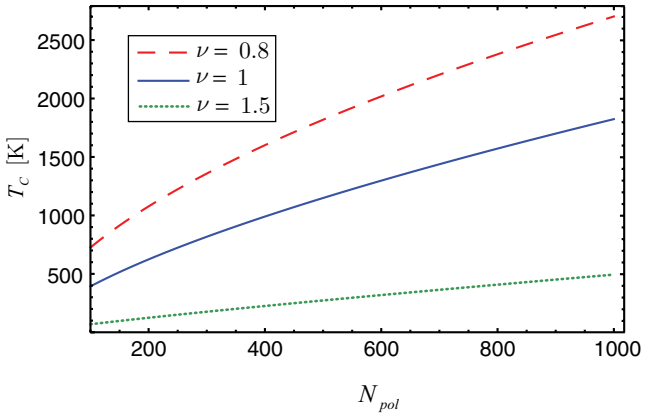

FIG. 5. (Color online) Critical temperature T_C versus number of polaritons $N_{\rm pol}$.

T_C as a function of LB polariton number $N_{\rm pol}$ is shown. A high-temperature BEC, as follows from Eq. (31) and Fig. 5, can be achieved for an experimentally feasible number of polaritons. Since the function $\zeta(x)$ diverges at $x = 2$ [see Eq. (31) and [3]], the critical temperature T_C vanishes for increasing trapping power parameter ν (see Fig. 5). From Eq. (31) we find a critical temperature which drastically increases with increasing α parameter. However, the values of the parameter are limited by inequality (2) for our problem.

Notably, the thermal de Broglie wavelength $\Lambda_T = [2\pi\hbar^2/(m_{\rm pol}k_BT)]^{1/2}$ at the experimentally explored temperatures of the atomic gas $T = 530$ K is macroscopically large (i.e., $\Lambda = 1.89$ μm) and comparable with the magnitude of characteristic length d_1 of photonic field localization.

IV. POLARITON BEC PROPERTIES AT $\nu = 1$

Let us examine LB polariton condensate properties at sufficiently "low" temperatures such as $T \ll T_C$, which is relevant to the linear trapping potential $U(z)$ obtained at $\nu = 1$. In this case the parameter $U_{\rm pol} = U(z)/|z|$ may be physically interpreted as a force acting on polaritons in the waveguide cavity. Macroscopic LB polariton BEC properties can be found with the help of a quantum field theory approach. In particular, the Lagrangian density L for the system described by Hamiltonian (26) looks like

$$L = \frac{i\hbar}{2}\left(\psi\frac{\partial\psi^*}{\partial t} - \psi^*\frac{\partial\psi}{\partial t}\right) + \frac{\hbar^2}{2m_{\rm pol}}\left|\frac{\partial\psi}{\partial z}\right|^2 + U_{\rm pol}|z||\psi|^2, \tag{33}$$

where $\psi(z,t) \equiv \langle\hat{\Xi}(z,t)\rangle$ is the classical polariton condensate ground-state wave function normalized as $\int_{-\infty}^{+\infty}|\psi(z,t)|^2dz = 1$. The Lagrangian density L implies the nonstationary Schrödinger equation for polaritons in *coordinate* representation in the form

$$i\hbar\frac{\partial\psi(z,t)}{\partial t} = \left[-\frac{\hbar^2}{2m_{\rm pol}}\frac{d^2}{dz^2} + U_{\rm pol}\,|z|\right]\psi(z,t). \tag{34}$$

To obtain a stationary solution we make the substitution $\psi(z,t) = e^{-i\mu t/\hbar}\psi(z)$, where μ is the chemical potential. Then we have

$$\frac{\hbar^2}{2m_{\rm pol}}\frac{d^2\psi(z)}{dz^2} + (\mu - U_{\rm pol}|z|)\psi(z) = 0. \tag{35}$$

The LB polariton ground-state wave function is expressed through the Airy function as (cf. [33])

$$\psi(z) = \frac{1.308}{\sqrt{d_{1,\rm pol}}}{\rm Ai}\left(\frac{|z|}{d_{1,\rm pol}} + a_1'\right), \tag{36}$$

where $d_{1,\rm pol} = [\hbar^2/(2m_{\rm pol}U_{\rm pol})]^{1/3}$ specifies a characteristic scale of spatial (longitudinal) localization of the polariton condensate for a linear trapping potential; $a_1' \approx -1.0188$ is the first zero of the Airy function derivative. It is interesting to note that the characteristic length $d_{1,\rm pol} = d_1$ is the same for the photons and photonlike polaritons trapped in the BWC due to the relation $m_{\rm pol}U_{\rm pol} = m_{\rm ph}U_{\rm ph}$; that is, true under condition (23) [see also Eqs. (17) and (28)]. Since LB polaritons are completely photonlike it is possible to conclude that the photon mode $n = 0$ reflects the behavior of polaritonic probability density $|\psi_n|^2 \equiv |\psi|^2$. The chemical potential μ can be easily found from Eqs. (35) and (36) and is given by

$$\mu = 1.0188U_{\rm pol}d_1. \tag{37}$$

To investigate the reaction of the BEC to a small disturbance induced from the outside we study the dynamics of the BEC when the initial wave function has been compressed or stretched compared to the equilibrium wave function. In this case one expects slow oscillations of the BEC around the equilibrium state. The dynamics of the polariton BEC induced by a disturbance can be found by means of the variational approach for solving Eq. (34). In particular, we take the Airy trial function for the ground state (cf. [34]):

$$\psi(z,t) = \frac{\mathbb{N}}{\sqrt{D(t)}}{\rm Ai}\left(\frac{|z|}{D(t)} + a_1'\right)e^{ib(t)|z|}, \tag{38}$$

where $\mathbb{N}$ is a normalization constant. In Eq. (38) the time-dependent function $D(t)$ specifies the width of the wave function, and $b(t)$ characterizes a related wave function curvature. Inserting Eq. (38) into Eq. (33) it is possible to obtain an effective Lagrangian $\bar{L} = \int_{-\infty}^{+\infty}Ldz$ by averaging Lagrangian density L as

$$\bar{L} = -\frac{2\hbar a_1'}{3}\frac{db}{dt}D - \frac{\hbar^2a_1'}{6m_{\rm pol}}\frac{1}{D^2} + \frac{\hbar^2}{2m_{\rm pol}}b^2 - \frac{2U_{\rm pol}a_1'}{3}D. \tag{39}$$

The effective Lagrangian $\bar{L}$ leads to a Newton-like equation for condensate width function

$$\frac{d^2D}{dt^2} = \frac{3\hbar^2}{4|a_1'|m_{\rm pol}^2D^3} - \frac{3U_{\rm pol}}{2|a_1'|m_{\rm pol}}. \tag{40}$$

For further processing it is useful to introduce a new dimensionless variable for the wave function width $w = D/d_1$ and the rescaled time $\tau = \omega_{\rm pol}t$, where $\omega_{\rm pol}$ is a characteristic frequency of polariton trapping defined as [cf. (16)]

$$\omega_{\rm pol} = \frac{\sqrt{3}\hbar}{2\sqrt{|a_1'|}m_{\rm pol}d_1^2} \simeq \left(\frac{3^{3/2}U_{\rm pol}^2}{2|a_1'|^{3/2}\hbar m_{\rm pol}}\right)^{1/3}. \tag{41}$$

The dimensionless equation for the new variables takes the form

$$\frac{\partial^2w}{\partial\tau^2} = \frac{1}{w^3} - 1. \tag{42}$$

The solution of Eq. (42) in the absence of polariton trapping is $w = (1+\tau^2)^{1/2}$, which describes the spreading of a free polariton wave packet with Airy shape (cf. [33]). In the presence of polariton trapping the analytical solution of Eq. (42) is much more complicated. Figure 6 demonstrates the temporal dynamics of the normalized polariton condensate wave function width w, using the rubidium parameters described in Sec. III (cf. [21–23]), which shows oscillations around the equilibrium solution. The characteristic frequency estimated for experimental conditions is $\omega_{\rm pol}/(2\pi) = 0.817$ THz. It is important that the value of $\omega_{\rm pol}$ should satisfy the quasiclassical condition (23) discussed above. Completely neglecting the decay rate, the polaritonic system exhibits periodical behavior similar to an atomic BEC in a harmonic trap (cf. [34]). The frequency $\Omega_{\rm osc}$ for small-amplitude oscillations (see Fig. 6)

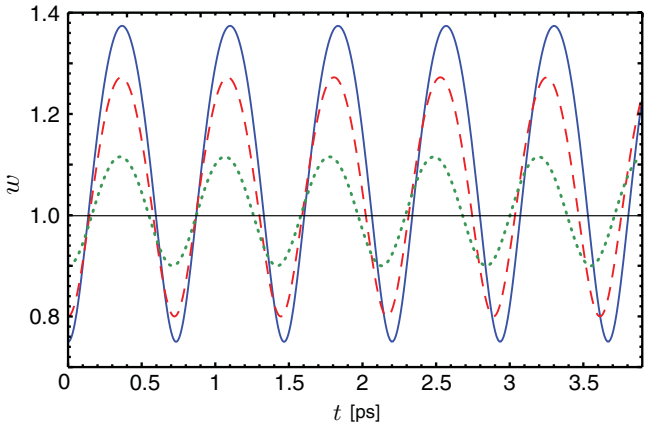

FIG. 6. (Color online) Normalized wave function width w versus time t. The parameters are the following: $\nu = 1$, $R_0 \approx 0.3$ μm, and $\alpha^{1/\nu} = 0.0005$ μm^{-1}. The initial conditions are $w(\tau = 0) = 0.75$ for the solid (blue) curve, $w(\tau = 0) = 0.8$ for the dashed (red) curve, and $w(\tau = 0) = 0.9$ for the dotted (green) curve. In all cases $\dot{w}(\tau = 0) = 0$. The horizontal line $w = 1$ corresponds to the stationary solution of Eq. (42).

can be obtained by linearizing Eq. (42) around the stationary state $w = 1$ and is found to be $\Omega_{\text{osc}} = \sqrt{3}\omega_{\text{pol}}$. The polariton wave function is stable everywhere in this case.

V. CONCLUSIONS

Let us briefly summarize the results obtained. We have considered the problem of the thermodynamics for polaritons emerging due to the interaction of two-level rubidium atoms with an optical field in the presence of OCs with buffer-gas particles. We assume the optical field to be trapped inside a biconical waveguide filled with rubidium atoms, and we find conditions for effective trapping of the coupled atom-light system. In particular, we find a phase transition to a BEC of polaritons if relation (23) is fulfilled, a condition that substantially depends on a cavity mode structure and α parameter characterizing slow changing of the waveguide radius along the longitudinal coordinate. We analyze the problem of BEC formation for lower-branch atomic polaritons trapped in the BWC under the quasiclassical approach (18) and (23), and we find that atomic polaritons formed in the waveguide may be treated as a 1D ideal gas of bosonic quasiparticles in the framework of current experimental results achieved for the thermalization of coupled atom-light states in the presence of a strong atom-field coupling regime.

Even though the character of the dressed-state polaritons discussed in the paper is nearly photonlike, they represent mixed states of photons and excitations of a two-level atomic system. In this sense they are physically close to exciton-polaritons obtained in semiconductor microcavities (cf. [12,13]). However, our estimations show that the critical temperature of the BEC phase transition can exceed the temperature of 530 K currently used in experiments, thus being high enough to be observed using appropriate waveguide parameters and cavity modes. Such high critical temperatures cannot be achieved for exciton-polaritons in current narrow-band semiconductor microstructures due to exciton ionization effects. The main reason for the high transition temperature is the photonlike character of the polaritons (i.e., their low effective mass). This, together with the thermalization due to optical collisions, may allow to experimentally observe a high-temperature phase transition of dressed-state polaritons using realistic parameters.

In a more detailed study we investigated the case of a biconical cavity leading to a linear trapping potential of a polariton gas. We are aware that the transverse decoherence rate needs to be studied in more detail for the considered system to ensure the strong-coupling limit. Using variational techniques we find the ground-state wave function to be Airy shaped, where the width w exhibits small-amplitude oscillations in time around a stationary state when the BEC is excited, with a characteristic period in the picosecond domain for current experiments. The results obtained indicate that the observation of a corresponding thermodynamic phase transition is possible already in current experimental setups, given the described waveguide structures are prepared with the required accuracy.

ACKNOWLEDGMENTS

This work was supported by RFBR Grants No. 10-02-13300, No. 11-02-97513, No. 12-02-97529, and No. 12-02-90419 and by the Russian Ministry of Education and Science under Contracts No. 16.518.11.7030, No. 2.4053.2011, and No. 3008.2012.2, and by the Deutsche Forschungsgemeinschaft (DFG) under Contract No. 436RUS113/995/0-1.

[1] E. H. Lieb and W. Liniger, Phys. Rev. **130**, 1605 (1963); E. H. Lieb, *ibid.* **130**, 1616 (1963); M. Girardeau, J. Math. Phys. (NY) **1**, 516 (1960).

[2] J. M. Kosterlitz and D. J. Thouless, J. Phys. C **6**, 1181 (1973); J. M. Kosterlitz, *ibid.* **7**, 1046 (1974).

[3] V. Bagnato, D. E. Pritchard, and D. Kleppner, Phys. Rev. A **35**, 4354 (1987); **44**, 7439 (1991).

[4] M. Bayindir, B. Tanatar, and Z. Gedik, Phys. Rev. A **59**, 1468 (1999); **59**, 4657 (1999).

[5] D. S. Petrov, D. M. Gangardt, and G. V. Shlyapnikov, J. Phys. IV France **116**, 7 (2004).

[6] V. A. Yurovsky, M. Olshanii, and D. Weiss, Adv. At. Mol. Opt. Phys. **55**, 61 (2008).

[7] H. Moritz, T. Stöferle, M. Köhl, and T. Esslinger, Phys. Rev. Lett. **91**, 250402 (2003).

[8] V. Dunjko, V. Lorent, and M. Olshanii, Phys. Rev. Lett. **86**, 5413 (2001); L. Salasnich, A. Parola, and L. Reatto, Phys. Rev. A **70**, 013606 (2004).

[9] M. Razeghi, *Technology of Quantum Devices* (Springer, Berlin, 2010).

[10] S. A. Moskalenko and D. W. Snoke, *Bose-Einstein Condensation of Excitons and Biexcitons and Coherent Nonlinear*

Optics with Excitons (Cambridge University Press, Cambridge, 2000).
[11] S. O. Demokritov *et al*., Nature (London) **443**, 430 (2006).
[12] S. Utsunomiya *et al*., Nature Phys. **4**, 700 (2008); A. Amo *et al*., *ibid*. **5**, 805 (2009).
[13] R. Balili, B. Nelsen, D. W. Snoke, L. Pfeiffer, and K. West, Phys. Rev. B **79**, 075319 (2009).
[14] M. Wouters, I. Carusotto, and C. Ciuti, Phys. Rev. B **77**, 115340 (2008); M. Wouters and I. Carusotto, Phys. Rev. Lett. **105**, 020602 (2010).
[15] O. A. Egorov, D. V. Skryabin, A. V. Yulin, and F. Lederer, Phys. Rev. Lett. **102**, 153904 (2009); O. A. Egorov, A. V. Gorbach, F. Lederer, and D. V. Skryabin, *ibid*. **105**, 073903 (2010).
[16] J. Klaers, J. Schmitt, F. Vewinger, and M. Weitz, Nature (London) **468**, 545 (2010).
[17] J. Klaers, F. Vewinger, and M. Weitz, Nature Phys. **6**, 512 (2010).
[18] J. Klaers, J. Schmitt, T. Damm, F. Vewinger, and M. Weitz, Phys. Rev. Lett. **108**, 160403 (2012).
[19] M. Fleischhauer and M. D. Lukin, Phys. Rev. A **65**, 022314 (2002); M. Fleischhauer, J. Otterbach, and R. G. Unanyan, Phys. Rev. Lett. **101**, 163601 (2008).
[20] E. S. Sedov, A. P. Alodjants, S. M. Arakelian, Y. Y. Lin, and R.-K. Lee, Phys. Rev. A **84**, 013813 (2011).
[21] U. Vogl and M. Weitz, Phys. Rev. A **78**, 011401(R) (2008).
[22] I. Yu. Chestnov, A. P. Alodjants, S. M. Arakelian, J. Nipper, U. Vogl, F. Vewinger, and M. Weitz, Phys. Rev. A **81**, 053843 (2010).
[23] U. Vogl, A. Sass, F. Vewinger, M. Weitz, A. Solovev, Y. Mei, and O. G. Schmidt, Phys. Rev. A **83**, 053403 (2011).
[24] A. P. Alodjants, I. Yu. Chestnov, and S. M. Arakelian, Phys. Rev. A **83**, 053802 (2011).
[25] B. M. Mashkovtsev, K. N. Tsibizov, and B. F. Emelin, *Waveguides Theory* (Nauka, Moscow, 1966) (in Russian).
[26] K. J. Vahala, Nature (London) **424**, 839 (2003).
[27] O. G. Schmidt and K. Eberl, Nature (London) **410**, 168 (2001); Y. F. Mei *et al*., Adv. Mater. **20**, 4085 (2008).
[28] R. F. Harrington, *Time-Harmonic Electromagnetic Fields* (Wiley, New York, 2001).
[29] M. Abramowitz and I. A. Stegun, *Handbook of Mathematical Functions with Formulas, Graphs, and Mathematical Tables* (National Bureau of Standards Applied Mathematics Series, Washington DC, 1972).
[30] Leonard I. Schiff, *Quantum Mechanics* (McGraw-Hill, New York, 1949).
[31] O. L. Berman, Yu. E. Lozovik, and D. W. Snoke, Phys. Rev. B **77**, 155317 (2008).
[32] Y. Louyer, D. Meschede, and A. Rauschenbeutel, Phys. Rev. A **72**, 031801(R) (2005); M. Pöllinger, D. O'Shea, F. Warken, and A. Rauschenbeutel, Phys. Rev. Lett. **103**, 053901 (2009).
[33] H. B. Thacker, C. Quigg, and J. L. Rosner, Phys. Rev. D **18**, 274 (1978); M. V. Berry and N. L. Balazs, Am. J. Phys. **47**, 264 (1979).
[34] V. M. Pérez-García, H. Michinel, J. I. Cirac, M. Lewenstein, and P. Zoller, Phys. Rev. Lett. **77**, 5320 (1996).